

Design Strategies of Fluorescent Dopant for Enhanced Photoluminescence Quantum Yield and Suppressed Dexter Energy Transfer

Jae Min Jang¹, Lee Da Yeon¹, Jang Ho Moon², Jun Yeob Lee^{1,2} *

¹ School of Chemical Engineering, Sungkyunkwan University

2066, Seobu-ro, Jangan-gu, Suwon, Gyeonggi, 16419, Republic of Korea

² Department of Display Convergence Engineering Sungkyunkwan University

2066, Seobu-ro, Jangan-gu, Suwon, Gyeonggi, 16419, Republic of Korea

E-mail : leej17@skku.edu

Abstract

In this work, we developed novel fluorescent materials, BFD01, BFD02, and BFD03, by incorporating a local unit with a low T_1 into the multiple resonance framework. BFD02 achieved a maximum external quantum efficiency of 8.6% in fluorescent devices by high photoluminescence quantum yield and BFD03 achieved an impressive external quantum efficiency of 18% in hyperfluorescence devices as a terminal emitter by suppressing Dexter energy transfer through bulky blocking groups.

Keywords

Blue device; Fluorescence; Hyperfluorescence; Organic light-emitting diodes

1. Objective and Background

Fluorescent materials with high photoluminescence quantum yield (PLQY) and good color purity along with high stability by attaining low triplet exciton energy have been widely studied. However, conventional fluorescence materials often suffer from poor color purity due to the presence of a noticeable vibration peak. This vibration peak arises from the structural relaxation between the ground state (S_0) and the singlet excited state (S_1), as well as from vibronic coupling in the S_1 . The vibronic coupling is enhanced by the bonding and antibonding characteristics of the highest occupied molecular orbital (HOMO) and the lowest unoccupied molecular orbital (LUMO) in polycyclic aromatic compounds.⁽¹⁾ Therefore, the strategy for developing novel fluorescence materials with suppressed vibrational peak is highly demanded.

In 2016, Hatakeyama et al. demonstrated a molecular design utilizing multi-resonance (MR) effect.⁽²⁾ This design induces separation of HOMO and LUMO within the atom, leading to short-range charge transfer (CT) and a unique electronic structure, resulting in high photoluminescence quantum yield (PLQY).^(1, 2) Additionally, the incorporation of a rigid molecular framework allowed high PLQY with narrow FWHM. Furthermore, the non-bonding character of the molecule effectively suppressed the appearance of vibrational peaks.

First, we successfully developed a purely fluorescent material, BFD01, by introducing a local unit with a low T_1 into the MR

framework. This approach achieved narrow FWHM while reducing the vibrational peak. Furthermore, the rigid configuration of MR framework successfully possessed high PLQY value. However, the low PLQY and the absence of bulky structure have intrigued the low efficiency of BFD01 in organic light-emitting diode (OLED) device.

In this work, we have successfully improved device efficiency by modulating BFD01 through introduction of absorption unit and blocking unit, respectively. As shown in **Figure 1**, the absorption unit implemented molecular BFD02 and bulky unit implemented molecular is BFD03. The BFD02 and BFD03 resulted in high radiative transition and high steric hindrance, respectively, which resulted in high PLQY and suppressed DET. These molecular design strategies have contributed to the high maximum external quantum efficiencies (EQE_{max}) of 8.6% and 7.9% in fluorescence OLED devices doped with BFD02 and BFD03, respectively, while BFD01 showed rather low EQE_{max} of 7.8%. To realize high efficiency, we have fabricated hyperfluorescence (HF) device by adopting 2',3',5',6'-tetrakis(3,6-di-tert-butyl-9H-carbazol-9-yl)-[1,1':4',1''-terphenyl]-4,4''-dicarbonitrile (p4TCzPhBN) as a sensitizer molecule. In HF device, BFD03 showed high EQE_{max} of 18%, while BFD01 showed low EQE_{max} of 16.4%. From the device results, we have demonstrated that the development of terminal dopant with high PLQY and large bulkiness is essential in realizing efficient OLEDs.

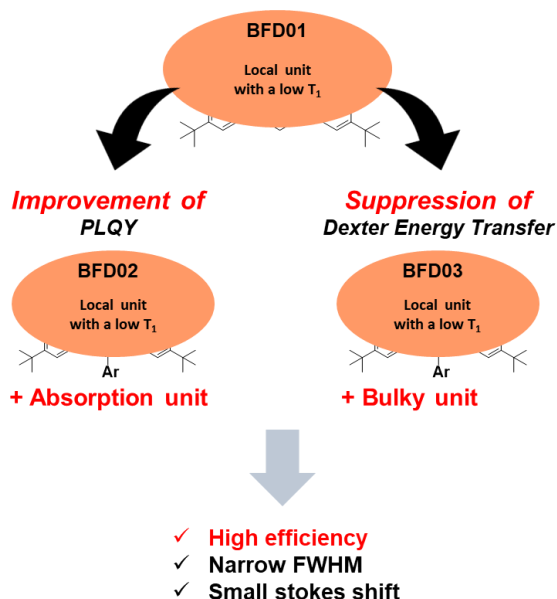


Figure 1. Design Strategy for the BFD Series for High Efficiency Tuning

2. Results

2.1 Photophysical properties

BFD01, a novel fluorescent material, was developed by incorporating a local unit with a low T_1 into the MR TADF framework. This design strategy maintained the advantages of MR frameworks such as lowered vibration peaks and high PLQY value while maintaining the fluorescent characteristic without delayed emission. However, the intrinsically low PLQY and the absence of bulky structure yield low efficiency in OLED device. Therefore, two strategic designs to achieve efficient fluorescent dopants were employed by adopting absorption unit and bulky unit in BFD01. The employment of absorption unit and bulky unit in BFD02 and BFD03 is expected to enhance PLQY and DET suppression capability when utilized as fluorescent dopant in OLED device.

Following the successful synthesis of the BFD series, purification was performed through column chromatography and recrystallization, with final purification achieved via sublimation. The photophysical and electrochemical properties were subsequently analyzed, as summarized in **Table 1**. Using a dilute and toluene tetrahydrofuran solution (1.0×10^{-5} M), ultraviolet-visible (UV-Vis) absorption and photoluminescence spectroscopy were utilized to measure the S_1 , triplet energy (T_1), and absorption spectrum (λ_{abs}). HOMO and LUMO energy levels were determined via cyclic voltammetry. The S_1 energy values of the dopants were 2.72, 2.71, and 2.70 eV, respectively, indicating the consistent use of the BFD01 core. These values were confirmed to be within an acceptable range. The HOMO, LUMO energy levels, and ΔE_{ST} are large in BFD series expecting not to contain delayed emission processes.

Table 1. Photophysical and electrochemical properties of BFD01, BFD02 and BFD03

	HOMO (eV)	LUMO (eV)	S_1 (eV)	ΔE_{ST} (eV)	Stokes Shift (nm)
BFD01	-5.46	-2.76	2.72	0.37	14
BFD02	-5.44	-2.72	2.71	0.43	13
BFD03	-5.42	-2.73	2.70	0.37	12

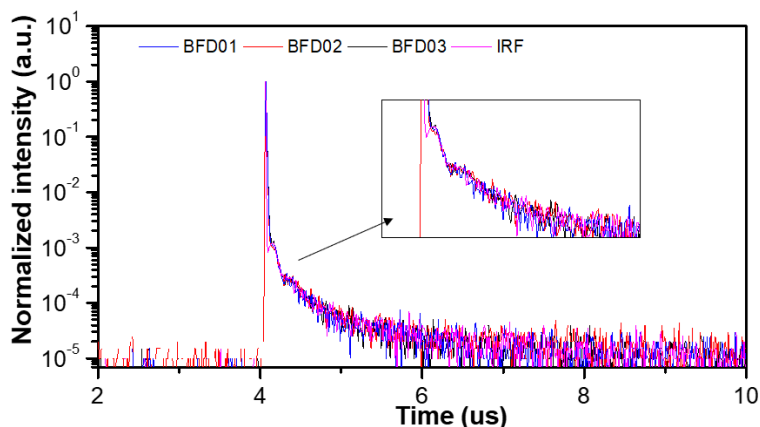


Figure 2. TRPL delay decay of BFD series with PMMA film

In **Table 1**, the UV-vis and PL data of BFD series reveal a suppressed vibronic peak and a small Stokes shift of 12 to 14 nm. These findings suggest that the MR characteristics of BFD01 are well-preserved, aligning with the intended design strategy, and may serve as critical factors for enhancing color purity. Transient PL decay (TRPL) measurements were conducted on polymethylmethacrylate (PMMA) films doped with 3 wt% of the dopants to analyze exciton decay profiles. The TRPL analysis in the film state confirmed that BFD01, BFD02, and BFD03 exhibit pure fluorescence properties without any delayed components **Figure 2**.

2.2 TRPL analysis

: PLQY increment & DET suppression

To evaluate the increase in PLQY caused by high radiative constant (k_r), TRPL measurements were performed on PMMA films doped with 3 wt% of the material, while the suppression of the DET process was evaluated through TRPL measurements on HF films. Additionally, PLQY measurements were conducted for BFD01 and BFD02 in 3 wt% doped PMMA films. BFD02 exhibited a significantly higher PLQY of 91.3%, compared to 65.3% for BFD01, and demonstrated a faster prompt decay than BFD01, as confirmed by TRPL measurements. These data are shown in **Figure 3(a)**. Photophysical parameters such as k_r was calculated from PLQY of prompt (Φ_F) and prompt decay rate constant (k_p) calculated from τ_p using equation reported previously.⁽³⁾ These findings suggest that BFD02 is likely to achieve higher efficiency when utilized in devices.⁽⁴⁾

To further evaluate the performance of BFD03, an EML film for HF devices was fabricated using bis[2-(diphenylphosphino)phenyl] ether oxide (DPEPO): p4tCzPhBN: 1 wt% fluorescent emitter. TRPL measurements conducted on HF EML films for BFD01 and BFD03 are shown in **Figure 3(b)**. BFD03 exhibited a delayed portion of 65%, whereas BFD01 displayed 57%. One possible explanation for the higher delay portion observed in BFD03 is the suppression of DET. These results suggest that BFD03 is capable of achieving improved efficiency in HF systems.⁽⁵⁾

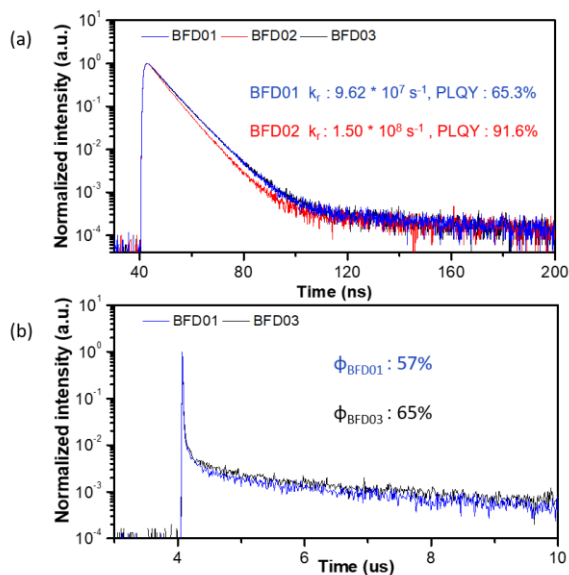


Figure 3. (a) TRPL prompt decay of BFD01 and BFD02 (b) TRPL delay decay of BFD01 and BFD03

2.2 Device Performance

To evaluate the device performances of the three fluorescent dopants, fluorescence devices were fabricated for the BFD series, along with HF devices for the BFD02 and BFD03 dopants. The structure of the fluorescence devices was indium tin oxide (ITO) (50 nm)/ Poly(3,4-ethylenedioxythiophene) polystyrene sulfonate (PEDOT:PSS) (40 nm)/ N-([1,1'-biphenyl]-4-yl)-9,9-dimethyl-N-(4-(9-phenyl-9H-carbazol-3-yl)-phenyl)-9H-fluoren-2-amine (BCFN) (10 nm)/ 9,9'-Diphenyl-9H,9'H-3,3'-bicarbazole (BCzPh) (10 nm)/ EML(25 nm)/ 2,4-diphenyl-6-(3-(triphenylsilyl)phenyl)-1,3,5-triazine (SiTrz) (5 nm)/ 2-[4-(9,10-Di-naphthalen-2-yl-anthracen-2-yl)-phenyl]-1-phenyl-1H-benzoimidazole (ZADN) (20 nm)/LiF (1.5 nm)/Al (200 nm). In the EML, 1-(3-(Phenanthren-1-yl)phenyl)-5-phenylanthracene (TTF-Phen) was used as the host, with a doping concentration of 1 wt%. The device structure is shown in **Figure 4**. Fluorescence devices based on BFD01 and BFD02 exhibited EQE_{max} values of 7.8% and 8.6%, respectively. The higher EQE_{max} of BFD02 can be explained by its enhanced PLQY and high k_r value, as identified in its PL characteristics. These results are considered reasonable and are summarized in **Table 2**.

Al(200)
LiF(1.5)
ZADN(20) / TPBi(10)
SiTrz(5) / TSP01(5)
Fluorescence device - TTF-Phen : BFD (25) HF device - DPEPO : P4tCzphBN : BFD (25)
BCzPh(10) / mCP(10)
BCFN(10) / TAPC(10)
PEDOT:PSS(40)
ITO(50)

Figure 4. Device structure of Fluorescence and HF, where Fluorescence is indicated in black and HF in red.

Table 2. Fluorescence and HF device properties of BFD01, BFD02 and BFD03.

	EQE ^[a] (%)	
	Fluorescence	HF
BFD01	7.8	16.4
BFD02	8.6	21.3
BFD03	7.9	18

[a] Data measured at maximum value.

To evaluate the DET suppression capability of BFD03, an HF device was fabricated with the structure indium tin oxide (ITO) (50 nm)/ Poly(3,4-ethylenedioxythiophene) polystyrene sulfonate (PEDOT:PSS) (40 nm)/ 1,1-Bis[(di-4-tolylamino)phenyl]cyclohexane (TAPC) (10 nm)/ 1,3-Bis(N-carbazolyl)benzene (mCP) (10 nm)/ EML (25 nm)/ Diphenyl-4-triphenylsilylphenyl-phosphine oxide (TSPO1) (5 nm)/ 1,3,5-Tris(1-phenyl-1H-benzimidazol-2-yl)benzene (TPBi) (10 nm)/ LiF (1.5 nm)/ Al (200 nm).

In the EML, DPEPO was used as the host, p4TCzPhBN as the sensitizer, and the terminal dopant was doped at 1 wt%. The device structure is shown in **Figure 4**. In fluorescence devices, BFD03 achieved an EQE_{max} of 7.9%, comparable to BFD01. However, in HF devices, the EQE_{max} values of BFD01 and BFD03 were 16.4% and 18%, respectively, with BFD03 exhibiting superior performance. These findings indicate that while the DET suppression strategy of BFD03 had minimal impact on fluorescence device efficiency, it significantly contributed to the efficiency enhancement of HF devices, enabling a higher EQE_{max}.

3. Impact of Research

In this work, new blue fluorescent dopants were designed, and the impact of molecular structure design on device efficiency was specifically analyzed, proposing a framework for high-efficiency device design. BFD02 and BFD03 achieved efficiencies of 8.6% and 18% in fluorescence and HF devices, respectively, demonstrating improved blue device performance compared to BFD01. BFD02 exhibited a high PLQY of 91.3% and rapid prompt decay, demonstrating excellent performance in fluorescence devices. BFD03 achieved superior efficiency in HF devices through its DET control strategy.

The comparison between HF devices and fluorescence devices provided a detailed understanding of how device structure and dopant design affect efficiency. This study successfully addressed the limitations of conventional fluorescent devices and offered a new pathway for advancing high-efficiency fluorescent OLEDs. By doing so, it enhanced the commercial feasibility of fluorescent OLEDs and laid the groundwork for further advancements in efficient fluorescent OLED development.

4. References

1. Kondo Y, Yoshiura K, Kitera S, Nishi H, Oda S, Gotoh H, et al. Narrowband deep-blue organic light-emitting diode featuring an organoboron-based emitter. *Nature Photonics*. 2019;13(10):678-82.
2. Hatakeyama T, Shiren K, Nakajima K, Nomura S, Nakatsuka S, Kinoshita K, et al. Ultrapure Blue Thermally Activated Delayed Fluorescence Molecules: Efficient HOMO-LUMO Separation by the Multiple Resonance Effect. *Advanced Materials (Deerfield Beach, Fla)*. 2016;28(14):2777-81.
3. Shin DJ, Hwang SJ, Lim J, Jeon CY, Lee JY, Kwon JH. Reverse intersystem crossing accelerating assistant dopant for high efficiency and long lifetime in red hyperfluorescence organic light-emitting diodes. *Chemical Engineering Journal*. 2022;446:137181.
4. Jeon SO, Lee KH, Kim JS, Ihn S-G, Chung YS, Kim JW, et al. High-efficiency, long-lifetime deep-blue organic light-emitting diodes. *Nature Photonics*. 2021;15(3):208-15.
5. Zhang D, Song X, Cai M, Duan L. Blocking energy-loss pathways for ideal fluorescent organic light-emitting diodes with thermally activated delayed fluorescent sensitizers. *Advanced Materials*. 2018;30(6):1705250.